

R.S. Booth, P.J. Diamond
Onsala Space Observatory
S-439 00 Onsala, Sweden
R.P. Norris
Nuffield Radio Astronomy Laboratories
Jodrell Bank, Macclesfield, Cheshire SK11 9DL, United Kingdom

ABSTRACT

Synthesis maps of stellar OH maser emission have revealed that the OH lies in expanding spherical shells typically about 10^{16} cm in diameter. From the maps and the expansion velocity, derived from the OH spectrum, stellar mass loss rates may be determined. Typical values are $10^{-5} M_{\odot}$ / yr. An important application of the stellar OH masers is in the estimation of stellar distances.

1. INTRODUCTION

Stimulated emission from the molecules OH, H₂O and SiO is found to be associated with late type, usually M, stars and supergiants, most of which are long period variables. Such stars are cool (photospheric temperatures ~ 2500 K) and have a large IR excess, indicating a dust envelope, which is attributed to mass loss. They are often detected only at IR wavelengths.

The OH masers associated with late type stars (or OH/IR stars) radiate most strongly in the 1612 MHz line of the ground state Λ -doublet, although weaker emission in the so called main lines at 1665 and 1667 MHz is not uncommon. The 1612 MHz spectrum consists of emission occurring in 2 sharply peaked velocity intervals spaced by between 10 and 30 km s⁻¹ (see Fig. 1) and many objects of this type have been discovered in 1612 MHz OH line surveys through their characteristic signature (e.g. Johanson et al., 1977).

A further important property of the OH emission is its variability, the line intensity being strongly correlated with the stellar light curve (in the case of identified objects) but having a phase lag of order 50 days (e.g. Harvey et al., 1974). This correlation indicates that the maser pump mechanism is intimately dependent on the stellar flux. In the case of the 1612 MHz sources there is a phase lag between the red and blue shifted OH peaks, an observation first reported by Shultz, Sherwood and Winnberg (1978).

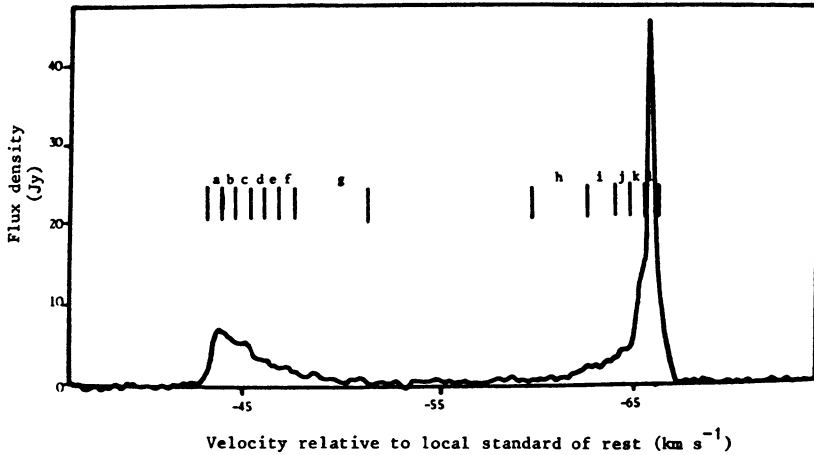


Fig. 1: 1612 MHz spectrum of OH 127.8-0.0.

The nature of the 1612 MHz spectral profile and the phase lag measurement strongly support the suggestion (e.g. Reid et al., 1977) that the OH emission comes from a spherical, uniformly expanding circumstellar shell. The strong outer spectral peaks are then the result of the high maser gain produced in the long constant velocity paths along the line of sight on the approaching and receding sides of the shell. If we assume that the OH emission is pumped by the stellar flux, then at all points in the shell it should emit and vary approximately in phase. However, at the earth we will observe a phase lag between the emission from different parts of the shell because of the difference in distance travelled by the emission. In particular the phase lag between the blue and red shifted peaks will give a direct measurement of the shell diameter.

The intensity of the maser emission observed from the earth will be a function of the coherent path length along the line of sight and will decrease with increasing shell radius. The observed emission should obey the expression

$$a(v) = r(1 - (v/v_e)^2)^{\frac{1}{2}}$$

where $a(v)$ is the shell radius at velocity v
 r is the overall shell radius
 and v_e is the expansion velocity of the shell.

At Jodrell Bank, combining data from three baselines of the radio linked interferometer network, we were able to confirm this prediction by making maps of the emission from OH 127.8-0.0 in several velocity intervals (Booth et al., 1981).

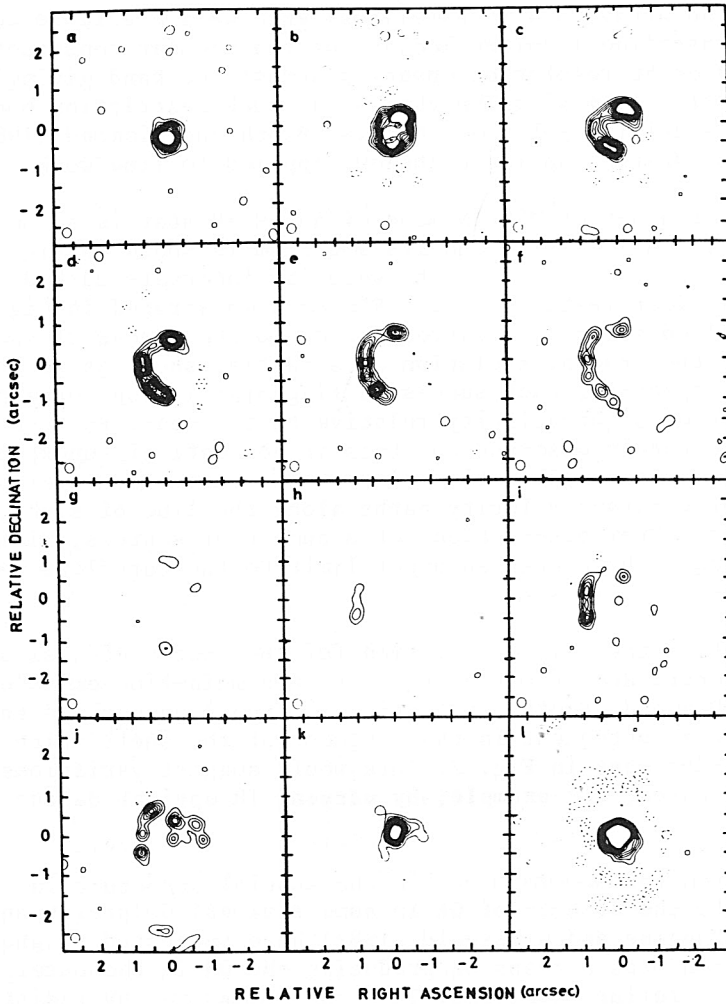


Fig. 2: MERLIN maps of the spatial distribution of the OH emission of OH 127.8-0.0 in the velocity intervals marked a to l in Fig. 1.

2. THE SPATIAL STRUCTURE OF THE OH EMISSION

During the past 2 years we have used the Jodrell Bank MERLIN instrument to map 16 OH/IR stars e.g. Norris, Diamond and Booth (1982) and Diamond et al. (in prep.). Complementary VLA measurements have been made by Spencer, Bowers and Johnston, (in prep).

Spectral line aperture synthesis is limited by the size of the correlator in the system since for each baseline we need a large number of delays in order to achieve a high frequency resolution. The MERLIN correlator currently has 1024 delays and so we limit the number of tele-

scopes in the array to 4 (6 baselines) when we are able to achieve 160 delays per baseline (limited because of the modular construction of the correlator) or 80 resolution channels across the band giving a typical resolution of $\sim 1 \text{ km s}^{-1}$. The VLA has no such restriction but it is limited in spatial resolution. Norris, Booth and Diamond (1982) have outlined the MERLIN mapping technique applied to line work.

An example of a set of MERLIN maps of an OH/IR star is shown in Fig. 2. The source is OH 127.8-0.0 and its spectrum is shown in Fig. 1. The individual maps correspond to the velocity intervals marked on that spectrum. Typical features of OH/IR maps demonstrated in Fig. 2 are the barely resolved structures corresponding to the strongest spectral peaks (a & 1) and the gradual evolution of a partial shell as we proceed through the spectrum, each successive ring of emission corresponding to a lower line of sight velocity relative to the star. Full shells of emission are rarely observed and this is not entirely unexpected since turbulence and streaming motions in the circumstellar envelope will break up the constant velocity paths along the line of sight, destroying coherence. From observations of a number of sources, Diamond et al. (in prep.) have shown that an upper limit to the turbulent velocity in the shell is $\sim 1.7 \text{ km s}^{-1}$.

This may not be the only explanation for the incompleteness of the shells, however. Recent observations of the main-line emission from OH 127.8-0.0 (Diamond, Booth and Norris, in prep.) have shown that 1667 MHz emission is strongest in that segment of the shell which is missing in the 1612 MHz maps in Fig. 2. This would suggest variations in pump conditions caused, for example, by varying IR optical depths in the shell.

A final reason for asymmetries in the spatial structure in the shells may simply be the absence of OH in some regions. Goldreich and Scoville (1976) and Huggins and Glassgold (1982) have suggested UV photodissociation of H_2O as a means of producing the OH in the outer regions of the circumstellar envelopes. Thus an asymmetric UV radiation field could cause the observed effect. Diamond, Norris and Booth (1983b) have attributed a major asymmetry in the NML Cygnus shell to enhanced OH production in the direction of the Cygnus OB association which is now believed to be at the same distance as NML Cyg. (see Morris and Jura, 1983).

Although expansion is the dominant dynamical process in the circumstellar shells, several maps show evidence of other dynamical effects e.g. rotation in OH 104.9 + 2.4 (Norris, Diamond and Booth, 1982) and Diamond (this volume) has evidence of a bipolar expansion in IRC 10420 (Diamond, Norris and Booth 1983a).

3. MASS LOSS

The MERLIN and VLA measurements referred to in section 2 have produced maps of 16 OH/IR stars. This data is summarized in Table 1. In general

TABLE 1: Properties of the OH/IR stars

Source	Distance (kpc)	Expansion veloc. (km s ⁻¹)	Shell radius (arcsec)	Mass loss rate ($\times 10^{-5} M_{\odot} \text{ yr}^{-1}$)
IRC10011	0.5(0.5)	19.3	4.4 [*]	2.5
OH127.8-0.0	5.8(3.3)	10.9	1.53	23.0
OH138.0+7.3	2.4	9.0	> 0.5	> 0.35
OH141.7+3.5	3.7	12.2	> 0.38	> 0.65
IRC50137	0.8	17.7	3.0 [*]	2.7
VYCMa	1.5	38.9	2.1 [*]	10.3
OH17.7-2.0	5.4	14.0	1.25	17.1
OH26.5+0.0	0.85(2.2)	14.8	3.25	3.0
OH32.8-0.3	3.2(4.3)	17.7	2.2 [*]	23.6
OH39.7+1.5	0.64(1.4)	17.0	2.0	0.75
R Aql	0.3	8.2	4.0 [*]	0.31
IRC10420	3.4	37.0	1.25	18.0
OH53.6-0.2	0.8	13.5	> 0.5	> 0.58
R RAql	0.9(0.4)	6.8	1.0 [*]	0.15
NML Cyg	2.0 (see text)	34/20 (double shell)	1.5/2.5	13.4
OH104.9+2.4	2.0(2.5)	14.3	1.44	3.2

Kinematic distances are given for the unidentified sources, except where a phase lag measurement of the shell linear diameter is available (Herman & Habing, 1981; Herman (private communication)). In that case the distance is estimated directly using the angular diameter measurement; the kinematic distance is then given in parenthesis.

Angular radii were measured with MERLIN (Norris et al., 1982, Diamond et al. 1982a,b and in prep., Chapman et al., 1983) and VLA (Spencer et al., in prep). VLA data is indicated with *.

Mass loss rates estimated as in section 3.

the circumstellar shells are shown to have angular diameters of a few arcsecs and linear radii $\sim 10^{16}$ cm. Since the expansion velocity v , is known from the OH spectrum, the mass loss rate, \dot{M} , can be calculated from $\dot{M} = 4\pi r^2 n v$ where r is the shell radius and n is the gas density. n may be estimated theoretically, e.g. Goldreich and Scoville (1976), and turns out to be $\sim 10^4$ cm⁻³ at these radii, giving $\dot{M} \sim 10^{-5} M_{\odot} \text{ yr}^{-1}$ in a typical case.

Such high mass loss rates cannot be supported for very long and so stars

in this evolutionary state must be short lived ($\sim 10^3$ yrs). Bowers, Johnston and Spencer (1981) have noted a correlation between the quantity rv^2 and mass loss rate, based on the requirement of a minimum OH optical depth for the maser process to occur. This correlation can thus be used to derive mass loss rates from the measured shell size and the expansion velocity.

4. DISTANCE MEASUREMENT

An important application of the OH mapping results is in the accurate determination of the distances to the OH/IR stars. Jewell et al. (1980) and particularly Herman and Habing (1981) have shown that by careful monitoring of the OH spectra the phase lag between the blue and red shifted emission peaks may be measured and a "light travel" shell diameter may be determined to $\sim 10\%$ accuracy. Dividing this by the shell's angular diameter measured with the interferometer gives the distance to the source. Herman (private communication) estimates that an overall accuracy of $\sim 10\%$ may be achieved. Since this is a direct estimate of distance involving no assumptions it will clearly become a valuable technique in the measurement of the galactic distance scale.

REFERENCES

- Booth, R.S., Kus, A.J., Norris, R.P., and Porter, N.D.: 1981, *Nature* 290, pp. 382-4.
- Bowers, P.F., Johnston, K.J., and Spencer, J.H.: 1981, *Nature*, 291, pp. 382-5.
- Chapman, J., Cohen, R.J., Norris, R.P., Diamond, P.J., and Booth, R.S.: 1983, *Mon.Not.R.Astr.Soc.* (in press).
- Diamond, P.J., Norris, R.P., and Booth, R.S.: 1983a, *Astron. Astrophys.* (in press).
- Diamond, P.J., Norris, R.P., and Booth, R.S.: 1983b, *Mon.Not.R.Astr.Soc.* (in press).
- Goldreich, P. and Scoville, N.: 1976, *Astrophys.J.*, 205, pp. 144-54.
- Harvey, P.M., Bechis, K.P., Wilson, W.J., and Ball, J.A.: 1974 *Astrophys. J.Suppl.* 27, pp. 331-57.
- Herman, J. and Habing, H.J.: 1981, *Physical Processes in Red Giants*, pp. 383-90 eds. Iben, I. and Renzini, A.
- Huggins, P.J. and Glassgold, A.E.: 1982, *Astr.J.*, 87, pp. 1828-35.
- Jewell, P.R., Weber, J.C., and Snyder, L.E.: 1981, *Astrophys.J.Lett.* 242, pp. L29-31.
- Johansson, L.E.B., Andersson, C., Goss, W.M., and Winnberg, A.: 1977, *Astron.Astrophys.Suppl.* 28, pp. 199-210.
- Morris, M. and Jura, M.: 1983, *Astrophys.J.* 267, 179-83.
- Norris, R.P., Booth, R.S., and Diamond, P.J.: 1982, *Mon.Not.R.Astr.Soc.* 201, 209-22.
- Norris, R.P., Diamond, P.J., and Booth, R.S.: 1982, *Nature* 299, pp. 131-4
- Reid, M.J., Muhleman, D.O., Moran, J.M., Johnston, K.J., and Schwartz, P.R.: 1977, *Astrophys.J.*, 214, pp. 60-77.
- Schultz, G.V., Sherwood, W.A., and Winnberg, A: 1978. *Astron.Astrophys.* 63, pp. L5-7.